Organic Process Research & Development **2009,** *13,* 114–124

Technology Reports

Use of a Fiber-Optic Turbidity Probe to Monitor and Control Commercial-Scale Unseeded Batch Crystallizations

Richard S. Harner, Roberta J. Ressler, Roger L. Briggs, James E. Hitt, Paul A. Larsen, and Timothy C. Frank*

The Dow Chemical Company, Midland, Michigan, U.S.A.

Abstract:

This article describes how a fiber-optic turbidity probe may be used as an inferential sensor to aid in the control of commercial-scale batch crystallizations. The discussion focuses on several unseeded crystallization examples involving cooling or cooling plus addition of antisolvent. In a typical control scheme, the fiber-optic probe is used to detect an initial nucleation event, to control a subsequent digestion step for fines dissolution with the potential for modification of nuclei size, number, and purity, and then to monitor a growth period. During the digestion step, temperature is increased and adjusted to achieve a desired reduction in the fiber-optic signal in order to control the extent of digestion. Within Dow, this approach has proven to be robust and cost-effective for numerous commercial-scale batch crystallizations including those with highly fouling or corrosive environments.

Introduction

Over a 20 year period, The Dow Chemical Company developed and has utilized an *in situ* fiber-optic turbidity probe to monitor and control commercial-scale batch crystallizations.[1−8] In this article, we describe the Dow methodology involving use of a simple and robust fiber-optic probe to control an unseeded crystallization process. Depending on the application, this methodology can provide a cost-effective means to achieving good results at the commercial scale. This can be particularly important for cost-sensitive applications such as production of generic actives or intermediates for which the cost of manufacture is a significant factor affecting commercial feasibility.

The fiber-optic probe measures backscattered light to generate a real-time turbidity signal indicative of the amount of solid-phase material present in the crystallizing slurry. It is used to infer the condition of the crystallization process rather than directly measure a specific property of the crystal mass. This inferential approach is similar in concept to the well-known use of temperature and pressure measurements to infer composition for cost-effective control of multicomponent distillation processes[9] and the use of inferential sensing techniques in general.[10] A number of probes that are more complicated than the fiber-optic probe may be used to obtain additional information, but these probes generally are more costly to install and maintain in the manufacturing environment. These include the focused beam reflectance measurement (FBRM) probe (with its rotating internal parts) used to measure crystal chord length distribution,[11] various video imaging probes used to determine crystal shape and size distribution,[12−14] as well as various spectroscopy probes including the attenuated total reflectance Fourier transform infrared (ATR-FTIR) probe[15−18] used to measure solute concentration in the mother liquor. Commercially available video imaging probes are similar to the fiber-optic probe

* Author for correspondence. E-mail: tcfrank@dow.com.

(1) Harner, R. S.; Gipson, N. D. Crystal Clear Batch: Fiber Optic Probe Helps to Control Batch Crystallizations in Pharmaceutical Applications. InTech, December, 2007.
(2) McLachlan, R. D.; Rothman, L. D. Fiber Optic Probe U.S. Patent 4,707,134, 1987.
(3) Chrisman, R. W.; McLachlan, R. D.; Harner, R. S. Method for Determining the Onset of Crystallization U.S. Patent 4,672,218, 1987.
(4) Harner, R. S.; Gutzmann, B. W. Sealed Fiber Optic Probe U.S. Patent 4,909,588, 1990.
(5) Harner, R. S. Dual Analysis Probe U.S. Patent 6,118,520, 2000.
(6) Harner, R. S.; Richardson, T. R.; Haney, K. L.; Bruck, T. R.; Chew, L. C. Fiber Optic Probes and Methods of Measuring Biological Materials U.S. Patent application, US2007081759 A1, 2007.
(7) Harner, R. S. Fiber Optic Technology for Process Monitoring and Control of API Manufacturing. ChE/Pharma 596 Seminar Series, University of Michigan, 2003.
(8) Cardis, T. M.; Goldman, D. S. Turbidity Applications with a Backscatter Fiber Optic Sensor In *Technical Papers of ISA*; Instrument Society of America: Research Triangle Park, NC, 2002; Vol. 428, pp 96−102. (This paper discusses a probe design licensed from The Dow Chemical Company.)
(9) Kano, M.; Miyazaki, K.; Hasebe, S.; Hashimoto, I. Inferential Control System of Distillation Compositions using Dynamic Partial Least Squares Regression. *J. Process Control* **2000**, *10*, 157–166.
(10) Kordon, A. K.; Smits, G. F.; Kalos, A. N.; Jordaan, E. M. Robust Soft Sensor Development Using Genetic Programming In *Nature-Inspired Methods in Chemometrics: Genetic Algorithms and Artificial Neural Networks*; Leardi, R., Ed.; Data Handling in Science and Technology, Vol. 23; Elsevier: Amsterdam, 2003; Chapter 3.
(11) Chew, J. W.; Chow, P. S.; Tan, R. B. H. Automated In-line Technique Using FBRM to Achieve Consistent Product Quality in Cooling Crystallization. *Cryst. Growth Des.* **2007**, *7* (8), 1416–1422.
(12) Larsen, P. A.; Rawlings, R. B.; Ferrier, N. J. Model-Based Object Recognition to Measure Crystal Size and Shape Distributions from In Situ Video Images. *Chem. Eng. Sci.* **2007**, *62*, 1430–1441.
(13) Wang, X. Z.; Roberts, K. J.; Ma, C. Crystal Growth Measurement Using 2D and 3D Imaging and the Perspectives for Shape Control. *Chem. Eng. Sci.* **2008**, *63*, 1173–1184.
(14) Li, R. F.; Penchev, R.; Ramachandran, V.; Roberts, K. J.; Wang, X. Z.; Tweedie, R. J.; Prior, A.; Gerritsen, J. W.; Hugen, F. M. Particle Shape Characterization via Image Analysis: From Laboratory Studies to In-process Measurements Using an in Situ Particle Viewer System. *Org. Process Res. Dev.* **2008**, *12* (5), 837–849.
(15) Lewiner, F.; Févotte, G.; Klein, J. P.; Puel, F. An On-line Strategy to Increase the Average Crystal Size during Organic Batch Crystallization. *Ind. Eng. Chem. Res.* **2002**, *41*, 1321–1328.

10.1021/op8001504 CCC: $40.75
Published on Web 12/10/2008

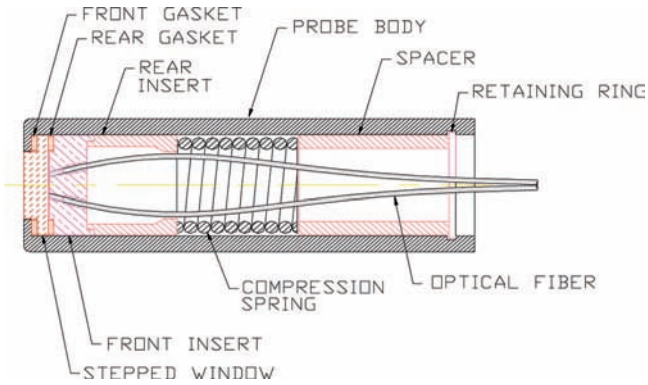

Figure 1. **Fiber-optic probe schematic.**

in the sense that many utilize backscattered light and most have no moving parts. However, at present they are more difficult to implement at the commercial scale due to their relatively bulky size and operating temperature limitations.

A fiber-optic probe can be used for a broad range of applications because the output signal depends only on the probe's ability to detect backscattered light; that is, no specific chemical properties such as molecular absorption are required. It also can be quite robust; numerous Dow probes have been in service for more than 10 years with no degradation in performance and without fouling problems. The basic Dow design includes a polished sapphire window, a spring-loaded gasket seal system to resist solvent infiltration, and fiber-retaining inserts (Figure 1). This design allows for expansion and contraction over a wide temperature range without breaching the process seal, yet it maintains precise optical alignment of the fibers and the window.[4] The potential for fouling is minimized due to the absence of flow-through channels that might be prone to plugging with solids and by designing the window so that it protrudes slightly from the probe tip to avoid crevices that might trap solids. A variety of probes that employ this basic design have been developed in Dow,[4−8] and a number of these are available from Guided Wave, Inc. (Rancho Cordova, CA, U.S.A.). Fiber-optic probes are also available from other suppliers including Mettler-Toledo Ingold, Inc. (Bedford, MA, U.S.A.).

To our knowledge, this article is the first to focus on the use of fiber optics in commercial-scale crystallizations. Al-Grafran et al.[19] reported using a fiber-optic probe along with other probes in a pilot-scale crystallization, and Ansari et al.[20] used a light scattering probe to monitor protein nucleation and crystallization in laboratory-scale hanging drop experiments. Control schemes that are similar to ours include methods described by Chew et al.[11] and by Lewiner et al.[15] These studies were carried out at the laboratory scale using other types of probes (FBRM or ATR-FTIR). In contrast with some other published approaches involving dissolution of fines throughout the batch crystallization process,[21−23] the fines dissolution or *digestion* methodology we describe normally modifies only an initial crop of primary-nucleated crystals, although multiple digestion steps can be employed. In principle, our methodology also may be applied to a seeded crystallization to modify the initial crystal mass prior to growth.

General Concepts

Turbidity. The classical definition of *turbidity* refers to the attenuation of light as it passes through a transparent medium containing dispersed particles.[24] Turbidity is caused by absorption and scattering mechanisms that reduce the amount of light traveling in a straight line. Scattering may be caused by solid particles, liquid drops, or gas bubbles dispersed within a liquid phase due to a difference in the index of refraction at the boundary between the dispersed and continuous phases. When a detector is placed in line with the incident beam (termed transmission mode detection), the transmittance of the sampled material often follows a Beer−Lambert relationship:

$$\frac{I}{I_o} = \mathrm{e}^{-\tau \times l} \qquad (1)$$

where transmittance is defined as the ratio of the measured intensity (I) to the intensity of the light source (I_o), τ is an empirically derived attenuation coefficient sometimes used to characterize turbidity, and l is the detected light's path length through the material. The value of τ is a function of particle size and concentration. For small particles at low concentrations it tends to vary in direct proportion to the concentration of scattering particles, but this relationship becomes nonlinear at sufficiently high concentrations. When the detector is placed at a 90° angle from the incident beam to directly measure the light scattered at this angle, the technique is called nephelometry. This configuration is particularly useful for measuring turbidity at low concentrations of solids because it involves

(16) Dunuwila, D.; Caroll, L. B.; Berglund, K. A. An Investigation of the Applicability of Attenuated Total Reflection Infrared Spectroscopy for Measurement of Solubility and Supersaturation of Aqueous Citric Acid Solutions. *J. Cryst. Growth* **1994**, *137*, 561–568.
(17) Wang, F.; Berglund, K. A. Monitoring pH Swing Crystallization of Nicotinic Acid by the Use of Attenuated Total Reflection Fourier Transform Infrared Spectroscopy. *Ind. Eng. Chem. Res.* **2000**, *39* (6), 2101–2104.
(18) Févotte, G. New Perspectives for the On-line Monitoring of Pharmaceutical Crystallization Processes Using in Situ Infrared Spectroscopy. *Int. J. Pharm.* **2002**, *241*, 263–278.
(19) Al-Grafran, M.; Andrews, J.; Dallin, P.; Gibson, N.; Grieve, N.; Hall, A.; Khan, S.; Ma, C. Y.; Mahmud, T.; Morris, J.; Ozkan, L.; Penchev, R. Y.; Price, C. J.; Roberts, K. J. Crystallisation of Organic Compounds at Supersaturation Closed Loop Control in a 250 Litre Industrial Pilot-Scale Batch Reactor7th World Congress of Chemical Engineering, Glasgow, UK, July 10−14. 2005.
(20) Ansari, R. R.; Suh, K. I.; Arabshahi, A.; Wilson, W. W.; Bray, T. L.; DeLucas, L. J. A Fiber Optic Probe for Monitoring Protein Aggregation, Nucleation and Crystallization. *J. Cryst. Growth* **1996**, *168*, 216–226.
(21) Jones, A. G.; Chianese, A. Fines Destruction During Batch Crystallization. *Chem. Eng. Commun.* **1987**, *62*, 5–16.
(22) Zipp, G. L.; Randolph, A. D. Selective Fines Destruction in Batch Crystallization. *Ind. Eng. Chem. Res.* **1989**, *28* (6), 1446–1448.
(23) Shan, G.; Igarashi, K.; Noda, H.; Ooshima, H. Production of Large Crystals with a Narrow Crystal Size Distribution by a Novel WWDJ Batch Crystallizer. *Chem. Eng. J.* **2002**, *85* (2−3), 161–167.
(24) Willard, H. H.; Merritt, L. L.; Dean, J. A.; Settle, F. A. *Instrumental Methods of Analysis*, 7th ed.; Wadsworth: New York, 1988.

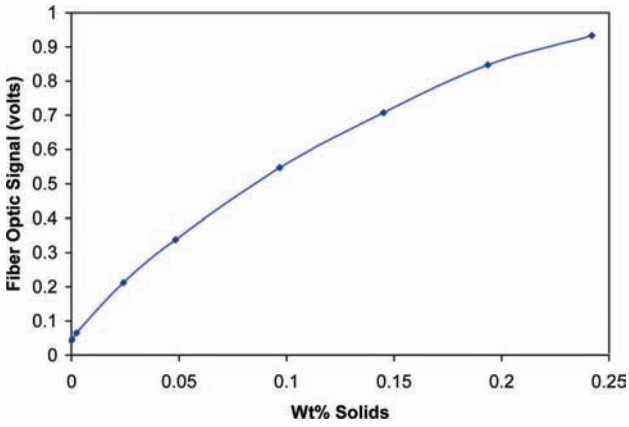

Figure 2. **Example fiber-optic signal versus particle concentration generated using 0.12 μm diameter polystyrene divinylbenzene beads suspended in water. The fiber-optic signal has been conditioned electronically to convert current from the photodetector circuit to voltage and then to amplify the resulting signal with a constant gain.**

a true zero background signal that enhances low-level detection. Backscattering is the term used to describe detection of light that is scattered approximately 180° back toward the light source. Like nephelometry, this configuration can generate a zero or near-zero background signal. The Dow probe incorporates a quasi-backscatter design using optical fibers such that both the light emission and detection fibers are mounted behind a window at the tip, allowing for a single-ended probe installation (Figure 1).

For precise characterization of turbidity, various standards are available for calibration including formazin-based materials and newer standards such as polystyrene divinylbenzene microbeads. For crystallization monitoring and control purposes, however, we simply record the output signal from the fiber-optic probe as an uncalibrated measure of particle concentration. The fiber-optic signal is also affected by particle size, temperature, liquid-phase composition, and to some extent, particle roughness and shape; thus, the signal provides only an approximate indication of relative particle concentration. The signal gain is initially adjusted for good response and to ensure that the turbidity signal does not exceed maximum output during any portion of the batch cycle. The same constant gain is then used for all subsequent batches. An example of fiber-optic signal output plotted versus the concentration of 0.12 μm diameter polystyrene divinylbenzene microbeads is shown in Figure 2. This plot simulates signal response at an early stage of crystallization.

Batch Crystallization Control Strategy. Production of crystals from solution is driven by generation of supersaturation, either by changing temperature, by evaporating solvent, by adding an antisolvent, or by reacting the feed solute with an added reagent to yield a less soluble reaction product. General reviews of crystallization phenomena and crystallization technology are available elsewhere.[25,26] The nucleation rate (often represented by an empirical power-law expression) normally dominates growth at high levels of supersaturation, while the growth rate (a more linear phenomenon) is the dominant rate at lower levels of supersaturation.[27] The rates of crystal nucleation and growth affect crystal purity as well as the crystal size distribution, because the number of crystals and the rate of crystal growth largely determine the number of crystal defects that are formed, either as mother-liquor inclusions or lattice defects. The critical supersaturation level at which nucleation begins to dominate can vary greatly from one system to another; however, in most cases, control of supersaturation by careful adjustment of process variables is required to meet desired specifications for the size and purity of product crystals.

Seed crystals may be added at the beginning of a batch crystallization to help control nucleation, although this adds complexity to the operating procedures, requires a process for preparing suitable seeds, and in the pharmaceutical industry, can complicate batch-to-batch traceability and record keeping. In some applications involving solutes that develop high levels of supersaturation before nucleating or when a specific polymorph is required, seeding may be necessary. However, in our experience with many applications involving crystallization of pharmaceutical intermediates and actives, agricultural chemicals, and other complex organic compounds, we have found that an unseeded protocol, as described in this article, often can be devised to meet customer requirements while avoiding the difficulties that seeding can present at a commercial scale. Unlike conventional unseeded protocols, the methodology we describe includes a digestion step that allows greater control of the *in situ* produced crop of nuclei. Digestion involves increasing the temperature or manipulating another process variable that affects solute solubility to modify the initial crystal population and supply the crystallizer with an appropriate number and purity of crystals for the remainder of the crystallization. Temperature and fiber-optic signal profiles for a typical cooling crystallization are shown in Figure 3. The fiber-optic signal profile shows an initial rise after nucleation followed by a decrease in signal during digestion. The extent of digestion can be characterized in terms of a corresponding reduction in fiber-optic signal relative to the maximum signal or peak height. This provides a means of conditioning the initial crystal mass in a repeatable manner such that improved results are achieved during the subsequent growth period. The probe can also be used during growth to match a desired rate of increase in the fiber-optic signal. Thus, the control strategy involves use of a fiber-optic probe to detect the onset of crystal nucleation and to provide a means of focusing on specific operational targets for digestion and growth periods. It can also compensate to some degree for normal variability in the feed composition, differences as to when nucleation occurs, and other batch-to-batch variations.

Normally a crystallization protocol and the corresponding fiber-optic profile are first developed in the laboratory. The

(25) Mullin, J. W. *Crystallization in the Process Industries*, 3rd ed.; Butterworth-Heinemann: Woburn, MA, 1997.
(26) Myerson, A. S., Ed., *Handbook of Industrial Crystallization*, 2nd ed.; Butterworth-Heinemann: Woburn, MA, 2002.
(27) Myerson, A. S.; Ginde, R. Crystals, Crystal Growth, and Nucleation In *Handbook of Industrial Crystallization*, 2nd ed.; Myerson, A. S., Ed.; Butterworth-Heinemann: Woburn, MA, 2002; Chapter 2.
(28) Falcon, J. A.; Berglund, K. A. Monitoring of Antisolvent Addition Crystallization with Raman Spectroscopy. *Cryst. Growth Des.* **2003**, *3* (6), 947–952.

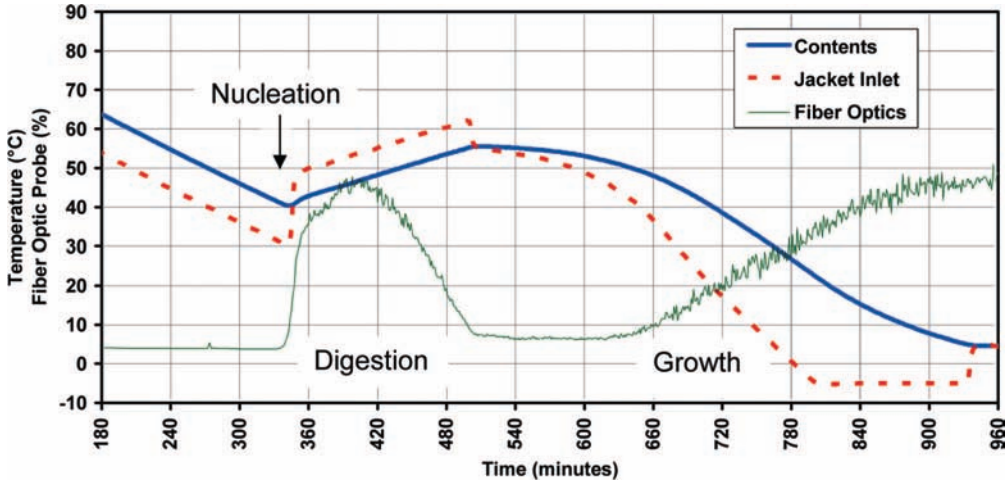

Figure 3. **Typical fiber-optic signal profile and temperature curves. The example is for cooling crystallization of Compound A using a commercial-scale (12,000 L) crystallizer. The fiber-optic signal is plotted as a percent of full scale first determined by setting the gain in an initial batch and then using the same constant gain for all subsequent batches.**

laboratory crystallizer may include a number of specialized probes in addition to a fiber-optic probe to aid in gaining a better understanding of the chemical system and to determine an effective protocol. These include the FBRM probe,[11] real-time video imaging,[12−14] and the ATR-FTIR probe mentioned earlier,[15−18] as well as the application of Raman spectroscopy.[28] In certain cases, the protocol that yields good results in the laboratory can then be implemented at the commercial scale using only the fiber-optic probe. In the examples given in this article, the main features of the fiber-optic profile determined in laboratory studies could be replicated at the commercial scale with similar crystallization results. As is well-known, however, some crystallizations can prove difficult to scale up no matter what control strategy and instrumentation are used due to sensitivities to changes in crystallizer capabilities related to the vessel's mixing characteristics or temperature control, and some crystallizations may require more sophisticated instrumentation to obtain desired crystal properties.[29,30] Furthermore, for a final pharmaceutical product it may be necessary to follow a crystallization operation with a milling operation to deagglomerate or adjust the final crystal size.[30]

Digestion. The digestion step can involve simple dissolution of the crystals or it can involve Ostwald ripening, in which case relatively large crystals grow larger at the expense of dissolving smaller crystals,[31,32] or both phenomena may play a role. The rate of simple dissolution is a function of the available solid surface area and the difference in Gibbs free energy (ΔG) between the solid and the dissolved solute such that[33]

$$\frac{\mathrm{d}\langle d^3\rangle}{\mathrm{d}t} \propto (\text{surface area}) \times f(\Delta G) \qquad (2)$$

where d represents an average particle diameter. For a crystallization involving change in temperature, the Gibbs free energy term in eq 2 may be approximated by the change in solute solubility, ΔX_i^{SAT}, obtained by heating the slurry. Ostwald ripening, on the other hand, is the phenomenon by which a population of crystals ages over time such that crystals smaller than a certain critical size become smaller or disappear, and crystals larger than the critical size grow larger.[27] It is driven by an increase in particle solubility as particle size decreases within this range. In the limit of low particle volume fraction and assuming no particle agglomeration occurs, the rate at which the average particle diameter increases is approximated by classical Lifshitz−Slyosov−Wagner theory such that

$$\frac{\mathrm{d}\langle d^3\rangle}{\mathrm{d}t} \propto \frac{\sigma V_m^2 C_i D}{RT} \qquad (3)$$

where σ is interfacial tension, V_m is the molar volume of solute i, C_i is the equilibrium solubility of i in the bulk liquid phase, D is the diffusivity of solute i in the liquid phase, R is the universal gas constant, and T is absolute temperature.[34−36]

For cooling crystallizations, digestion normally is carried out by slowly heating a crystal slurry for a period of time, or

(29) Fujiwara, M.; Nagy, Z. K.; Chew, J. W.; Braatz, R. D. First-principles and Direct Design Approaches for the Control of Pharmaceutical Crystallization. *J. Process Control* **2005**, *15*, 493–504.
(30) Variankaval, N.; Cote, A. S.; Doherty, M. F. From Form to Function: Crystallization of Active Pharmaceutical Ingredients. *AIChE J.* **2008**, *54* (7), 1682–1688.
(31) Ostwald, W. *Analytische Chemie*, 3rd ed.; Engelmann: Leipzig, 1901; p 23.
(32) Ostwald, W. On the Supposed Isomerism of Red and Yellow Mercury Oxide and the Surface Tension of Solid Substances. *Z. Phys. Chem.* **1900**, *34*, 495–503.
(33) Lüttge, A. Crystal Dissolution Kinetics and Gibbs Free Energy. *J. Electron Spectrosc. Relat. Phenom.* **2006**, *150*, 248–249.
(34) Lifshitz, I. M.; Slyosov, V. V. The Kinetics of Precipitation from Supersaturated Solid Solutions. *J. Phys. Chem. Solids* **1961**, *19* (1−2), 35–50.
(35) Wagner, C. Theory of Precipitate Change by Redissolution. *Z. Elektrochem.* **1961**, *65*, 581–591.
(36) Lindfors, L.; Skantze, P.; Skantze, U.; Rasmusson, M.; Zackrisson, A.; Olsson, U. Amorphous Drug Nanosuspensions. 1. Inhibition of Ostwald Ripening. *Langmuir* **2006**, *22*, 906–910.

optionally by heating and holding the crystallizer at a constant temperature, to modify crystal size and population. This may also result in significant purification of the crystal mass. An example is described by Cobley et al.[37] for purification of (*R*)-2-methylenesuccinamic acid crystals suspended in isopropanol. In this example, heating the agitated crystal slurry to 40 °C and holding for an hour increased purity from 98.0% ee to >99.5% ee. Ostwald ripening may be particularly important for purification because overall purity will increase if the number of defects present in the new growth of larger crystals is less than that in the dissolving fines. Moreover, for some applications, an additional degree of purification may be achieved due to an annealing-like effect similar in concept to the "sweating" step used to purify a crystal mass produced by crystallization from the melt.[38] With sweating, a degree of crystal purification is achieved due to rejection of impurities as crystals are partially melted, washing the remaining crystal mass of mother liquor residue and to some extent reducing crystal defects through annealing.

The relative rates at which these processes occur can vary, depending on the system, but it is expected that in many cases the relative rates are likely to order as follows: dissolution > Ostwald ripening ≫ annealing. The rate of annealing due to solute diffusion in solid phases is extremely slow; however, solute diffusion along solid-phase boundaries may be sufficiently fast to play a role, particularly for those applications in which the initial crystal mass is produced with a fair number of impurity-rich defects such as mother-liquor inclusions caused by rapid nucleation.

Growth Period. During the growth period of a cooling crystallization, the process often is controlled so that the temperature rate of change increases as the batch is cooled in a near-parabolic cooling curve. Figure 3 shows a typical example. This is done partly because at lower temperatures the change in solubility that results from a given step change in temperature typically is less than that obtained at the higher starting temperature. Also, the batch can tolerate higher cooling rates while still favoring growth as more and more solute comes out of solution and the total crystal surface area available for growth increases. Use of an increasing-rate cooling curve is a well-known strategy for minimizing cycle time.[39] Similar strategies may be useful for other types of crystallizations involving different ways of generating supersaturation.

Mixing Characteristics and Scale-Up. An important aspect that needs to be considered for scale-up is the kind of mixing that can be achieved in the large-scale crystallization vessel. We have obtained good results on scaling from 4 L in the laboratory up to volumes as large as 12,000 L in the plant using high-volume, low-shear axial-flow mixing impellers for good circulation with minimal secondary nucleation or crystal breakage or attrition. Although this magnitude of scale-up can be risky and is not appropriate for all applications, the use of the fiber-optic probe can help to reduce the scale-up risk. Guidelines for good mixing design within crystallizers are given elsewhere.[40−42] In addition to its effect on crystallization phenomena and the heat-transfer capability of a jacketed vessel, the mixing design should ensure that the probe, which normally is inserted through a dip pipe that enters the vessel from the top, is sensing a representative volume of the vessel contents. Additionally, the signal response can change, depending on the direction the fiber-optic probe is pointed relative to the flow field. Finally, it should be understood that satisfactory mixing is not always achieved in a commercial-scale vessel, particularly in glass-lined vessels that typically are under-baffled and often utilize nonoptimal agitator designs. Careful attention to modifying the mixing characteristics of an existing vessel often is warranted.

Compounds and Equipment

Compounds. Batch crystallization results are reported for various proprietary organic compounds manufactured using multistep batch processing methods typical of the pharmaceutical and specialty chemical industries. These compounds, identified in this article only as Compounds A−D, are complex organics with molecular weights in the range of 150−600 g/mol.

Equipment. Crystallizations were carried out using well-mixed jacketed stirred-tank vessels with batch volumes of 1 L to 12,000 L. The specific sizes and operating conditions used to crystallize the various solutes are described in Examples. The data were generated using various Dow-designed fiber-optic backscatter probes. The probe design details are given elsewhere.[1−4] In typical installations, a 0.500 in. (12.7 mm) diameter probe was installed through a dip pipe that entered the crystallizer vessel from the top, typically through a 4 to 8 in. diameter nozzle for a 12,000 L (3000 gal) vessel. Engineering calculations for stress and mechanical moment[43] were used to specify a dip pipe design strong enough to withstand the bending forces generated in the crystallizer. Many different dip pipe configurations may be used including free-standing heavy-wall dip pipes or concentric dip pipes (a pipe within a pipe) or dip pipes integrated into baffle-plates for support. In other applications, a combined fiber-optic probe and temperature sensor[5] may be inserted through a thermowell nozzle at the side of the vessel or into a circulation loop.

Examples

Cooling Crystallization Strategies. Figure 3 shows the fiber-optic signal profile and corresponding temperature versus

(37) Cobley, C. J.; Lennon, I. C.; Praquin, C.; Zanotti-Gerosa, A.; Apell, R. B.; Goralski, C. T.; Sutterer, A. C. Highly Efficient Asymmetric Hydrogenation of 2-Methylenesuccinamic Acid Using a Rh-DuPHOS Catalyst. *Org. Process Res. Dev.* **2003**, *7* (3), 407–411.

(38) Ulrich, J.; Bülau, H. C. Melt Crystallization In *Handbook of Industrial Crystallization*, 2nd ed.; Myerson, A. S., Ed.; Butterworth-Heinemann: Woburn, MA, 2002; Chapter 7.

(39) Rawlings, J. B.; Sink, C. W.; Miller, S. M. Control of Crystallization Processes In *Handbook of Industrial Crystallization*, 2nd ed.; Myerson, A. S., Ed.; Butterworth-Heinemann: Woburn, MA, 2002; Chapter 9.

(40) Paul, E. L.; Midler, M.; Sun, Y. Mixing in the Fine Chemicals and Pharmaceutical Industries In *Handbook of Industrial Mixing: Science and Practice*; Paul, E. L., Atiemo-Obeng, V. A., Kresta, S. M., Eds.; Wiley: Hoboken, NJ, 2004; Chapter 17.

(41) Atiemo-Obeng, V. A.; Penney, W. R.; Armenante, P. Solid Liquid Mixing In *Handbook of Industrial Mixing: Science and Practice*, Paul, E. L., Atiemo-Obeng, V. A., Kresta, S. M., Eds.; Wiley: Hoboken, NJ, 2004; Chapter 10.

(42) Green, D. Crystallizer Mixing: Understanding and Modeling Crystallizer Mixing and Suspension Flow In *Handbook of Industrial Crystallization*, 2nd ed.; Myerson, A. S., Ed.; Butterworth-Heinemann: Woburn, MA, 2002; Chapter 8.

(43) Dally, J. W.; Riley, W. F. *Experimental Stress Analysis*; McGraw-Hill: New York, 1978; p 20.

Table 1. **Batch crystallization results for Compound A**

batch number	digestion	crystallizer batch size, total weight (kg)	crystallization batch time (h)	filtration time (h)	specific filtration time (min/kg feed slurry)	wetcake moisture content (wt %)	final crystal assay (%)
1	no	389	13.4	48.3	7.46	25	95.5
2	no	580	11.7	14.0	1.30	12	99.3
3	yes	548	17.6	6.0	0.54	6	99.9+
4	yes	579	12.5	3.6	0.26	4	99.9+
5	yes	907	14.6	5.0	0.16	3	99.9+
6	yes	877	15.5	3.5	0.13	3	99.9+

time curves for a commercial-scale cooling crystallization of Compound A. In this example, the goal was to produce easily filtered crystals with good purity while minimizing the total batch cycle time including filtration. The process was begun with the batch held at a temperature that assured complete dissolution of the feed material. Cooling the solution at about 8 C°/h gave good nucleation results. This cooling rate was achieved in the manufacturing plant by controlling the vessel's jacket temperature at a constant ΔT of 10 C° below the contents temperature. Controlling the jacket ΔT generally is preferred over direct control of the contents temperature to avoid large ΔTs and wall temperatures that are either too cold or too hot (depending on the point in the batch cycle), because this can cause unwanted nucleation or fouling at the wall and severely limit the jacket's heat transfer capability. When the fiber-optic signal began to rise, indicating that nucleation had occurred, the batch was then heated at a rate of 6 C°/h to begin the digestion step. This heating rate was accomplished by controlling the jacket temperature at a ΔT of 7 C° above the contents temperature. Heating was continued until a desired reduction in the fiber-optic signal was obtained. As shown in Figure 3, the signal rose from about 3% output to about 45% output during nucleation. Digestion was stopped at about 9% output, when about 85% of the rise in signal due to nucleation (above the 3% baseline) had been reduced. At that point, a slow cooling profile was begun to generate a level of supersaturation sufficiently low to promote crystal growth and production of easily filtered crystals, yet not so slow as to require an unnecessarily long period of time in the crystallizer. In general, the appropriate cooling curve can be determined in laboratory-scale experiments, or with the aid of a fiber-optic probe, can be developed and optimized at full production scale.

Table 1 summarizes the results achieved by crystallizing Compound A at the commercial scale. Batches 1 and 2 were made using a parabolic cooling profile without a digestion step and without the aid of a fiber-optic probe. Batches 3−6 were made using the probe to facilitate a digestion step as described above, followed by a cooling curve similar to the one used for the initial batches. The temperature curve used to crystallize Batch 1 is shown in Figure 4. This poorly controlled crystallization yielded small crystals that were dark in color and high in impurities, and the resulting slurry was difficult to filter on a standard centrifuge, requiring two days to finish. In comparison, the better-controlled batches yielded larger, lighter-colored crystals, and significantly higher purity. These batches filtered and deliquored easily and quickly, as indicated by a dramatic decrease in filtration cycle time and a much lower moisture content of the filter cake (Table 1).

These results, as well as the results we have obtained with other crystallizations, show that the digestion methodology can be used to affect both particle size and purity of the final product. They also show how the use of digestion in an appropriate control scheme, even one that increases the crystallizer batch time, can yield a dramatic reduction in the overall cycle time including filtration. In general, the basic control scheme may be adapted to modify the properties of a given crystalline product within certain limits. If higher purity is needed, more digestion is carried out, followed by a slower growth curve. If smaller crystals are desired, the extent of digestion is reduced, and a faster cooling curve is used. Also, a hold step may be added during digestion to provide additional time for Ostwald ripening.

Another cooling crystallization profile, this one designed to generate small crystals of Compound B, is shown in Figure 5.

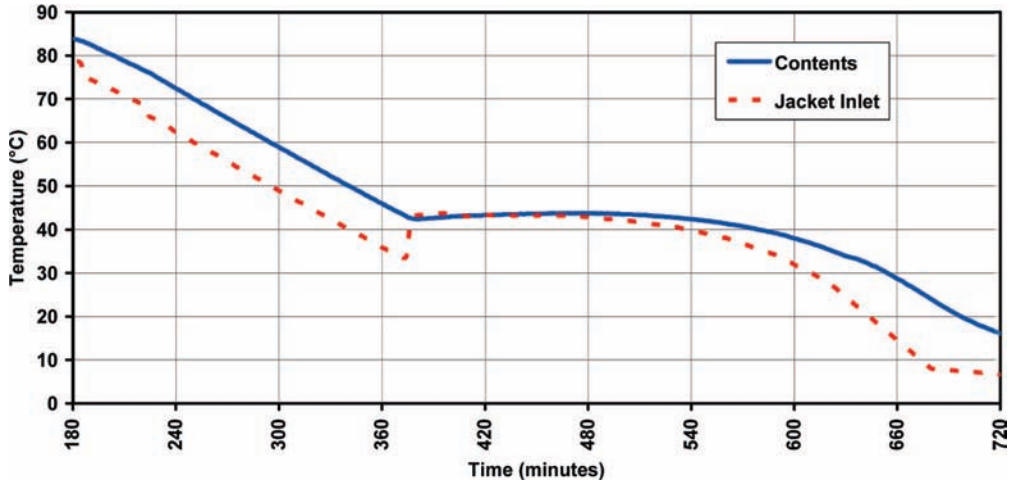

Figure 4. **Unseeded Compound A crystallization profile (12,000 L scale) without use of a fiber-optic probe and no digestion step.**

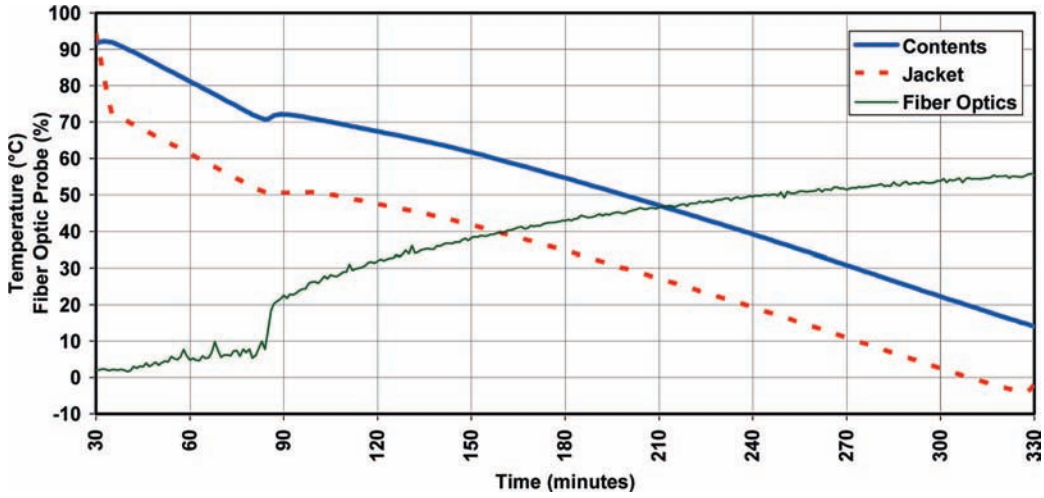

Figure 5. **Typical fiber-optic signal profile and temperature curves for cooling crystallization of Compound B in a commercial-scale (12,000 L) crystallizer.**

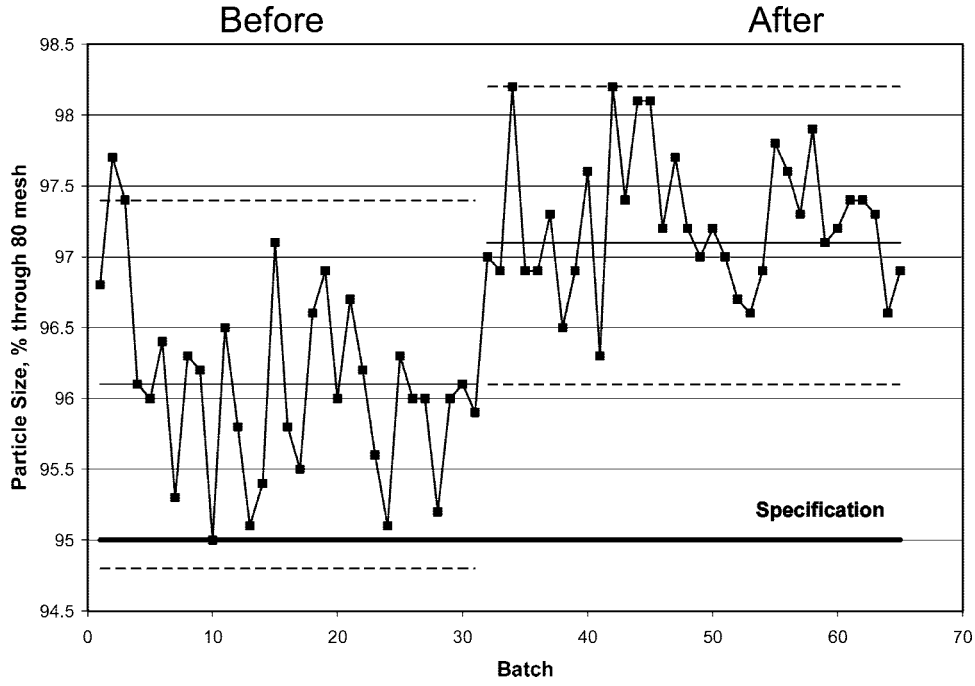

Figure 6. **Impact of enhanced crystallization control on commercial plant capability to reproducibly meet particle size specification for Compound B. Results are after milling. The dotted lines are the upper and lower control limits. Solid lines represent the mean values. After implementing the new control scheme, all batches were well above the specification that 95+% of sampled material will pass through an 80 mesh screen.**

This crystallization was implemented primarily to adjust the final product's crystal size distribution. Higher purity was not the primary goal in this case, because most of the required product purification had already been accomplished in an upstream operation. In this case, the profile that gave the desired results did not require a digestion step. The cooling profile could be initiated immediately following nucleation, as soon as this was detected by the fiber-optic probe. The results of implementing the profile shown in Figure 5 are summarized in Figure 6. In this example, the percentage of particles after milling that would pass through an 80 mesh screen in a quality control test at the plant could be brought into much better control. This allowed the plant to more reliably meet the customer's specifications.

Effect of Scale on the Fiber-Optic Signal Profile and Final Crystallization Results. In the next example involving cooling crystallization of Compound C, we provide more detailed information about the crystallization and show how the main features of a desired fiber-optic signal profile can be replicated on scale-up to obtain similar crystallization results (Figures 7 and 8). This example illustrates replacement of a seeded crystallization protocol with an unseeded one and demonstrates robust particle size reproducibility on scale-up from 1 L to

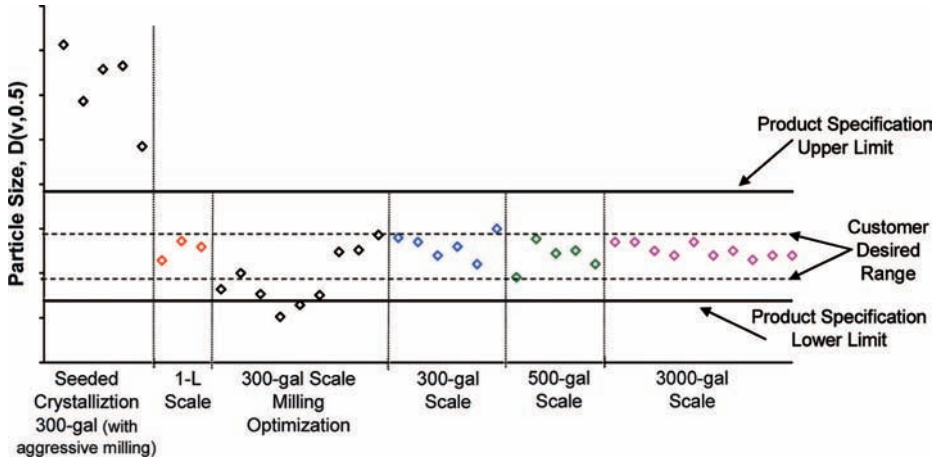

Figure 7. **Particle size results corresponding to Figure 8, after mild milling to break agglomerates (Compound C). Each data point corresponds to a different batch. Particle size was determined using a Malvern Mastersizer 2000 particle size analyzer. Representative samples were dispersed in water using a surfactant. Particle shape was roughly spherical, so the volume mean diameter was chosen as a convenient measure of crystal size.**

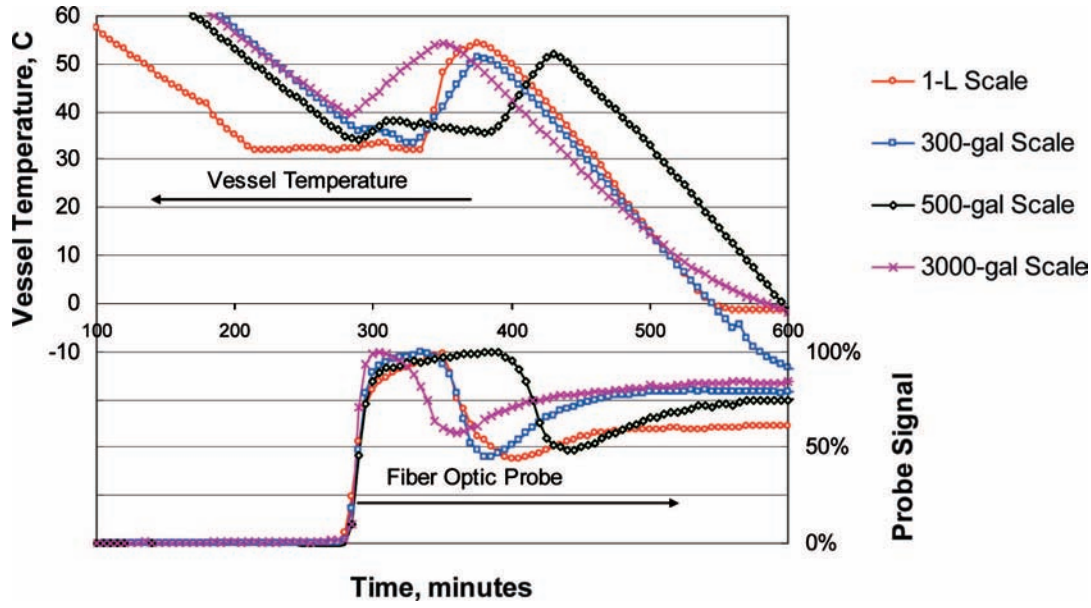

Figure 8. **Typical cooling curves and fiber-optic signal profiles at various scales (Compound C).**

12,000 L (3000 gal). In this case, crystallization was followed by a mild milling operation to break up agglomerates.

An existing seeded crystallization protocol involved initiating nucleation by seeding at a specified temperature, waiting for the relief of supersaturation, and then ramping down the temperature to a final set point, thus growing the mass of crystals that developed after seeding the batch without any modification. This procedure produced large and reasonably pure crystals; however, much smaller (yet still pure) crystals were needed for the final product formulation. A milling study showed that the aggressive energy input necessary to reduce particle size to the desired target (beyond breaking agglomerates) would melt the compound in a standard impact mill. This unsuccessful attempt is labeled "Seeded Crystallization 300-gal (with aggressive milling)" in Figure 7. In response to this situation, an effort was initiated to develop a new crystallization procedure that could produce smaller crystals and still achieve the necessary purification while also eliminating the use of seeds. The initial cooling ramp was extended and followed by a holding period if needed to allow for spontaneous nucleation. A heat-back digestion step was included following nucleation to control particle size and improve purity. Subsequent adjustment of the digestion parameters allowed precise control of particle size within the desired range. The 1 L scale work served as the proof-of-concept to justify further development work at the 300-gal scale which was needed to demonstrate and optimize the deagglomeration milling operation at 1/10th the commercial scale. The same crystallization protocol developed at the 1 L scale was used at the larger scales; only the milling parameters were varied in the "300-gal Scale Milling Optimization" time period shown in Figure 7. This period of milling optimization was the only time during which out-of-specification particle size was produced with the unseeded crystallizer control strategy.

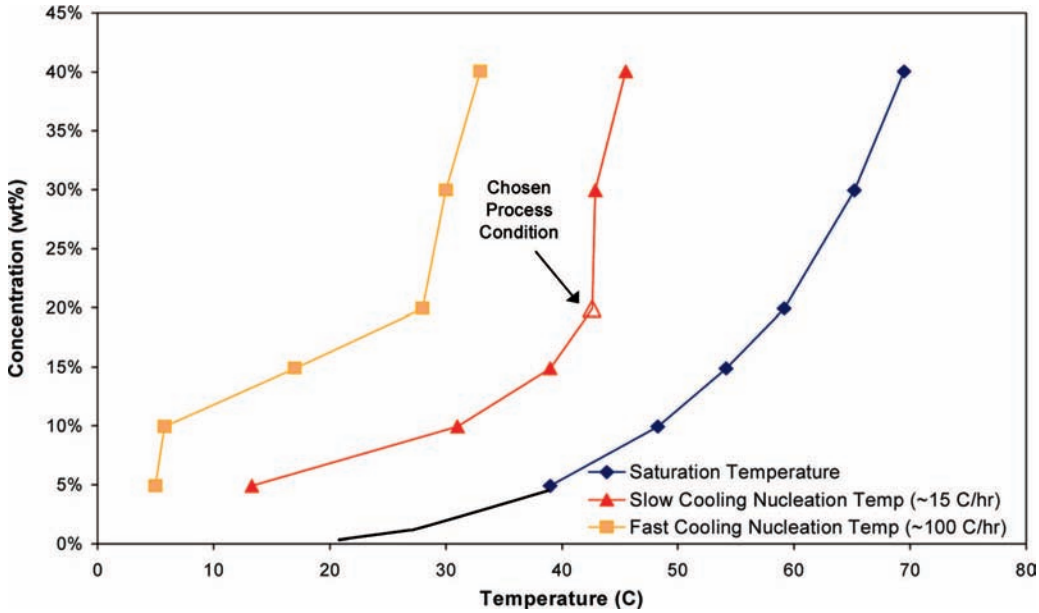

Figure 9. **Solubility and metastable zone width for Compound C.**

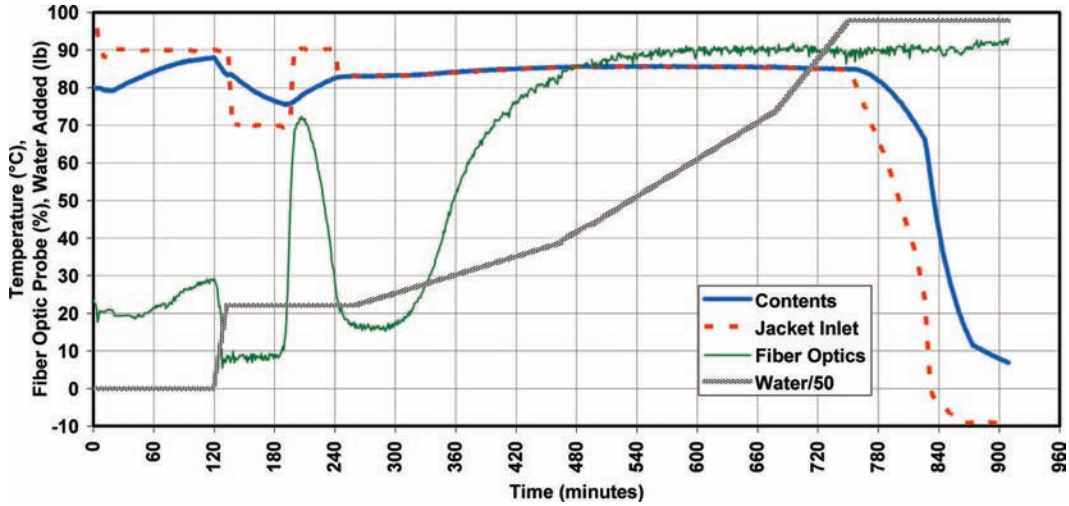

Figure 10. **Crystallization of crude Compound D from ethanol/water at the 3000 gal scale to achieve desired purity and filterability. For addition of water, the amount has been divided by 50 to fit the scale.**

Typical signal profiles and heating/cooling curves used to crystallize Compound C are shown in Figure 8 for the different scales of operation. These cooling curves allowed high recovery of the product compound and good productivity per batch, since the solubility of the product is reasonably high at the starting temperature and low at the final temperature (Figure 9). The data provided in Figure 9 also illustrate the metastable zone width for this application. Starting with a product concentration of 20 wt % and an initial cooling rate of about 15 C°/h to induce nucleation gave good results. The fiber-optic probe enabled precise control of digestion by (1) detecting the nucleation event, (2) providing a measure of the number of nuclei produced (in terms of a subsequent rise in the fiber-optic signal), and (3) providing a measure of the degree to which heating the batch during digestion reduced the number of nuclei (in terms of a resulting decrease in the fiber-optic signal). The target dissolution was taken to be 50% of the increase in fiber-optic signal following nucleation. Once that target was achieved, the cool down was begun, resulting in growth of the adjusted crystal mass. In preparing Figure 8, the fiber-optic probe signals were zeroed and normalized to the same maximum value to provide a convenient indication of the degree to which the 50% dissolution goal was achieved during digestion. Clearly there is variation within this small set of data. The process actually ran with 40−60% reduction of the fiber-optic probe signal, but this variability did not significantly affect the final results, as shown in Figure 7. The use of a digestion step in this procedure not only yielded a more tightly controlled particle size distribution, but also resulted in faster filtration rates, a factor that is particularly important for production of products requiring small crystal size.

Finally, as the process was scaled up, the use of the fiber optic probe allowed some compensation for differences in nucleation points as well as differences in the

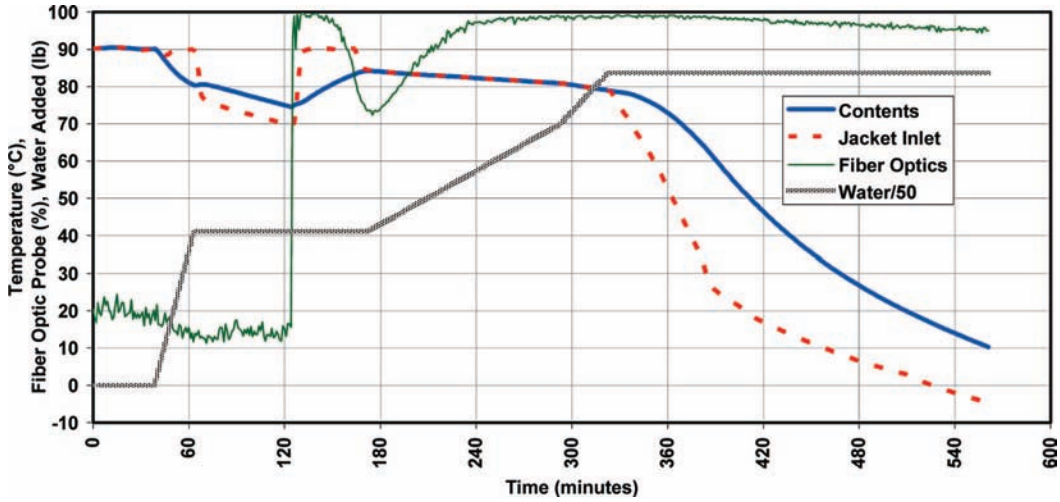

Figure 11. **Crystallization of Compound D product from ethanol/water at the 3000-gal scale to achieve desired specific surface area. For addition of water, the amount has been divided by 50 to fit the scale.**

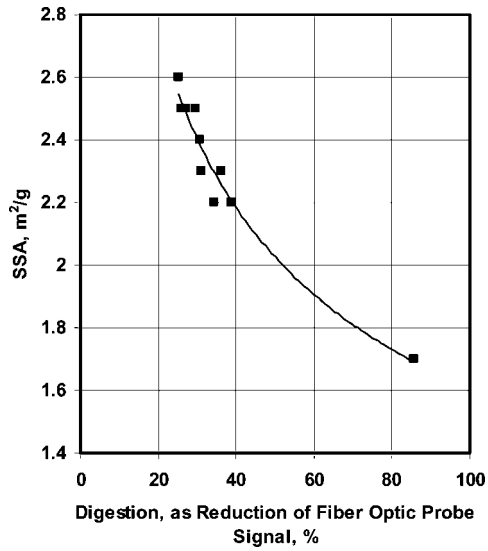

Figure 12. **Compound D specific surface area as a function of the extent of digestion.**

heat transfer capabilities and mixing intensities at the different scales. In Figure 8, the temperature curves and fiber-optic signal profiles have been plotted so they all align at a point in time corresponding to the initial nucleation event. This represents the start of the crystallization and helps to highlight some of the differences between these batches. Note that the temperatures at which nucleation occurred were not the same in each case: 1 L scale at 32 °C; 300-gal scale at 40 °C; 500-gal scale at 36 °C; and 3000-gal scale at 42 °C. Thus, spontaneous nucleation generally occurred sooner (at a higher temperature) as scale was increased, and this is representative of our experience with all the batches. This may be due to an increase in the maximum shear rate experienced by the batch as scale was increased due to use of higher power per unit volume to maintain the crystal suspension. In any case, the fiber-optic probe could be used to adjust the process to compensate for these differences. Regarding differences in heat transfer capabilities, in this example the 1 L laboratory-scale batch was heated at the fastest rate during digestion and the 3000-gal commercial-scale batch was heated at the slowest rate, with the other scales in between. This was due to a decrease in heat transfer capability with increasing size of jacketed vessel. Similarly, the temperature curve for the 3000-gal scale did not decrease as fast as the others toward the end due to the larger vessel's lower heat-transfer capability. This particular system was able to tolerate all of these differences with little effect on the final results. Furthermore, in Figure 8 the different fiber-optic signal profiles do not line up exactly in the same region of the plot because of differences in the time taken between the detection of nucleation and the start of heating for digestion. The profile for the 500-gal batch in particular stands out with an extended wait step. This extra time was simply due to a need to wait for the operator to complete other more pressing activities. This profile was included in Figure 8 to further illustrate how the profile could vary and still yield the desired results.

Application to Antisolvent-Addition Crystallization. Controlling a batch crystallization to achieve a desired fiber-optic signal versus time profile is a strategy not limited to cooling crystallizations but can be applied to other types of crystallization as well. An example involves two crystallizations used in the manufacture of Compound D at the 12,000 L (3000 gal) scale. In this case, the product was crystallized from solution in ethanol by addition of water as an antisolvent as well as by cooling. Addition of the antisolvent improved product recovery by reducing product solubility to lower levels than could be achieved by cooling alone. The first crystallization was carried out to achieve the desired crystal purity, and this was followed by a second crystallization or recrystallization to control specific surface area (SSA) to meet final product specifications for a product that was not milled downstream. Specific surface area was measured using the Brunauer–Emmett–Teller (BET)

method[44] to characterize crystal size, because the product compound formed a needle-shaped crystal, and obtaining a direct measure of particle size was problematic. Also, it is important to note that implementing crystallizations involving addition of antisolvent or for reactive crystallizations involving the addition of a reagent, the mixing achieved in the large-scale crystallizer can have a dramatic effect on the results.[45] In these cases, successful application of the fiber-optic probe control methodology requires that careful attention is given to the design of mixing equipment in order to obtain good results on scale-up. In this example, the water was added through a dip pipe near the tip of an axial flow impeller for rapid dispersal of the antisolvent.

In the first crystallization of crude Compound D (Figure 10), a predetermined amount of the antisolvent (water) was added early in the batch, while Compound D was in solution. After the initial water addition, the batch was cooled to nucleation and then digested by heating. Then, a water addition profile was followed, adding the antisolvent more slowly at first and then more rapidly. During this antisolvent addition step, the jacket temperature was set equal to the contents temperature. After the water addition was complete, a near-parabolic cooling profile was followed. For the final product crystallization (Figure 11), a similar control scheme was followed, but the digestion was less substantial, and the water addition rate was faster (Figure 11). This yielded smaller crystals with the required specific surface area. The relationship between specific surface area and the extent of digestion in terms of the change in fiber-optic signal is shown in Figure 12.

Summary

We have provided examples illustrating the use of a fiber-optic turbidity probe to monitor and control unseeded batch crystallization processes. The probe is used to detect an initial nucleation event, to control a subsequent digestion step designed to modify the initial crop of crystal nuclei, and then to monitor a crystal growth period. The general control strategy involves adjustment of process variables that affect generation of supersaturation to match a desired fiber-optic signal versus time profile or pattern. The extent of digestion can be characterized in terms of the reduction in fiber-optic signal observed during the digestion step. The initial crop of nuclei may be conditioned in a repeatable manner by focusing on a specific operational target quantified in terms of a desired change in the fiber-optic signal relative to the maximum signal value observed after nucleation is first detected. One of the examples we discuss (for Compound C) also shows how the probe can aid in the scale-up of a crystallization process.

Acknowledgment

We gratefully acknowledge Nick Gipson, Pat Gipson, and Mark Nitz for many valuable discussions and thank Alison Beatty and Earl Soules for supporting this work.

Received for review June 25, 2008.

OP8001504

(44) Brunauer, S.; Emmett, P. H.; Teller, E. Adsorption of Gases in Multimolecular Layers. *J. Am. Chem. Soc.* **1938**, *60*, 309–319.

(45) Frank, T. C.; Fort, W. S.; Jones, C. M. Treat Precipitation Reactions as Reactive Crystallizations. *Chem. Processing* **2005**, *68* (12), 37–41.